Biokinetics of Radiolabeled Monoclonal Antibodies in Heterotransplanted Nude Rats: Evaluation of Corrected Specific Tissue Uptake

Christian Ingvar, Kristina Norrgren, Sven-Erik Strand, Thomas Brodin, Per-Ebbe Jönsson, and Hans-Olov Sjögren

Departments of Surgery, Lund and Helsingborg, Radiation Physics and Wallenberg Laboratory, Lund University, S-221 85 Lund, Sweden

A tumor model is presented to study the biokinetics and localization of radiolabeled monoclonal antibodies (MAb) in the nude rat (Rowett RNu/RNu) heterotransplanted with human melanoma metastases. The nude rat is larger, less sensitive, and lives longer than the nude mouse. It is, therefore, well suited for in vivo studies of tumor localization with radiolabeled monoclonal antibodies. The tumor-to-host weight ratio was closer to the human situation for the nude rat than for the mouse, and quantitative imaging could be performed with a parallel hole collimator. We followed the antibody biokinetics for as long as 8 days, with repeated blood sampling and imaging. Specific uptake of MAb was higher in tumor tissue than in all other tissues except blood. Initial high uptake was also recorded in the bone marrow. The lymph glands showed a slow uptake of specific and control antibody. A simple in vitro correction procedure is described to calculate the corrected specific tissue uptake (STU_{corr}) that takes the blood activity into account. Thus it was shown that 80% of the tissue uptake in the dissected liver at 30 hr was due to labeled antibodies circulating in the blood. The specific tissue uptake ratio of antibodies 96.5 and OKT3 (nonspecific control) was unity for all other organs except for tumor tissue, where the ratio was greater than two and even higher when correction for blood content of labeled antibody was made.

J Nucl Med 30:1224–1234, 1989

A successful application of monoclonal antibodies (MAb) for radioimmunoimaging and therapy of human tumors, regardless of tumor localization, requires a proper knowledge of the kinetics of the MAb distribution, the affinity of the antibody to the antigen, and its localization.

New monoclonal antibodies are continuously introduced, and a reliable and reproducible animal model for in vivo testing is urgently needed. The nude mouse is very susceptible to low grade infections and surgical procedures are difficult to carry out (*1*). An optimal experimental animal should be large enough to discriminate well between tissue areas for quantitative scintillation camera imaging, tolerate repeated blood sampling, surgical manipulations, and selective injections of monoclonal antibodies. In addition, it is desirable that detailed biokinetics can be evaluated including, i.e., the lymph nodes and the bone marrow, necessary for compartment analysis and absorbed dose calculations, and that a correction for the blood content of labeled antibody in tissues could be made.

Different in vivo animal models for testing tumor antibody specificity have been published (*2–7*). All these models use the heterotransplanted nude mouse. However, in most human studies with radiolabeled antibodies, the highly promising results from experiments in the nude mice could not be reproduced (*8–11*). The tumor uptake of antibodies was much lower in patients than in the nude mouse and the tumor-to-background ratio was relatively low, often less than two.

In this paper we present the basic data for our nude rat model that overcomes much of the difficulties in the nude mouse model.

It is crucial to define accurately the type of uptake that is evaluated in the experiments. In most papers, the specific tissue uptake (STU) reported consists of a sum of the corrected specific tissue uptake (STU_{corr}) and the activity present in the blood. We describe here

Received Aug. 9, 1988; revision accepted Feb. 29, 1989.

For reprints contact: Christian Ingvar, MD, Dept. of Surgery, Lund University, S-221 85 Lund, Sweden.

a simple correction method to evaluate the corrected specific tissue uptake in our nude rat model.

MATERIAL AND METHODS

The Nude Rat

Nude rats (Rowett RNu/RNu strain), 2-3 mo of age, with a weight of 210 ± 25 g were used (*12*). The rats are bred and kept in cages with filter taps and provided with autoclaved feed pellets, sterilized drinking water ad libitum, and sterile wood granulate bedding in a temperature controlled unit receiving particle filtered air. During the experiments (~1 wk), the rats were kept outside the sterile atmosphere in special cages with an air filter. The animals were anesthetized with ether and 0.5-1 ml of blood was withdrawn from the periorbital venous plexa four to five times during the week, without any signs of negative effects.

Tumor

A tumor biopsy was taken from a patient with melanoma metastases. Under sterile conditions the tumor was cleaned from connective and necrotic tissue and put into sterile Ringer solution. The tumor specimen was then meshed into a cell suspension that was injected at different locations in the animal. Tumor growth was established by serial passages in the rat. The tumors reported here are all from the same passage and all animals received a tumor on each thigh; intramuscularly (right) and subcutaneously (left). In general, the tumor growth was locally invasive without any distant tumor spread. In this study animals were injected with antibodies 1 wk after tumor inoculation when the tumor was just palpable.

Monoclonal Antibody

The monoclonal antibody reported here was the 96.5 (IgG 2a) specific for p97, a cell surface glycoprotein with the molecular weight of 97,000, present in 60-80% of human melanoma but only in trace amounts in normal tissues (*13*). (MAbs supplied by Drs. Ingegerd and Karl-Erik Hellström, Oncogen, Seattle, WA) Antibodies were purified from ascites fluid of mice, bearing hybridoma ascites tumors, by affinity chromatography on a Protein A Sepharose CL-4B column (Pharmacia Uppsala, Sweden) with a stepwise pH gradient elution (*13,14*). The purity of the monoclonal antibodies were estimated by agarose electrophoresis. The antibodies were stored at −70°C.

Monoclonal antibody OKT3 (IgG1, specific for T-cell antigen, not present in these nude rate lacking thymus) was used as a nonspecific control (*15*).

Immunohistochemical Assay

The binding of mouse monoclonal antibodies to antigens, expressed in xenografts of human melanoma in the nude rat, was demonstrated in a modified biotin-avidin based immunohistochemical assay (*16*). Briefly, the primary antibody was incubated on frozen tissue sections for 1 hr. This and successive incubations were performed at room temperature. After washing the sections, the second biotinylated antibody was incubated for one-half hour. To reduce background staining as a result of the presence of endogenous rat Ig in the tissue, a monoclonal rat anti-mouse Ig (light chains) antibody was used in this step. The sections were washed again and a streptavidin biotinylated peroxidase complex was added and incubated for one-half hour. After washing, the substrate solution (diaminobenzidine) was added and sections incubated for 15 min. The sections were washed with ether, dried and mounted directly or counter stained with Giemsa before counting.

Antibody Labeling

The monoclonal antibody 96.5 (350 μg) was labeled with 37 MBq iodine-125 (^{125}I) (the iodine solution contained 3×10^{16} iodine ions per ml), using the Chloramine-T method (*17*). By elution on a Sephadex G 25 column (Pharmacia PD 10) the peak fractions of labeled protein were eluated and used for the experiments. The labeling efficiency of the ^{125}I 96.5 MAb was 70%. The antibody was labeled with less than one iodine atom per molecule, thus not interfering with the immunoreactivity (*18*). The antibody OKT3 (300 μg) was labeled accordingly with ^{131}I (25 MBq).

Cell Binding Assay

The binding of the labeled antibodies to a suspension of cultured melanoma cells H-1477 (Mel-28) was tested by the direct binding assay described by Brown et al. (*15*). Briefly, 2×10^6 trypsinized melanoma or control cells were incubated with 20 ng of labeled antibody in 100 μl of PBS (phosphate buffered saline) with 1% BSA (bovine serum albumin) and 0.01% NaN_3 for 1 hr at 0°C. Cells were washed twice and bound activity counted. The antibody activity of the labeled protein was expressed as the ratio of bound and total added activity. By preceding titrations it was shown that the number of cells used represented a large antigen excess. The binding of labeled antibody to cultured melanoma cells (Mel 28), was 62%, implicating that the binding capacity to the melanoma antigen p97 was retained.

Red Blood Cell Labeling

The blood volume was calculated by technetium-99m (^{99m}Tc) labeling of red blood cells (RBC) in vivo (*19*) and determined postmortem in the different tissue samples. Four hours before the animal was killed, the RBC labeling was performed by i.v. injection of 0.5 μg Sn^{2+} ion solution (10 mg $SnCl_2$ diluted in 10 ml saline with HCl at pH 2.0). After 10 to 15 min incubation, $^{99m}TcO_4^-$ (10 MBq) (freshly eluated) was injected intravenously. Labeling efficiency was 90%, determined by measuring the ^{99m}Tc activity in the red blood cells and in the plasma, 15-30 min after injection.

Experimental Design

Through a groin incision, the superficial femoral vein was exposed and punctured, and the labeled antibodies were injected, thus minimizing extravascular deposits. The mean amount of antibody 96.5 injected was 45 μg (40-49 μg), which corresponds to ~5 MBq ^{125}I and for OKT3, injected separately, 26.5 ± 7 μg corresponding to 0.5 MBq. Blood samples were taken from the periorbital venous plexa at regular intervals and the plasma and red blood cells were separated by centrifugation. The rats were killed at different times (6 -200 hr) following the injection of labeled antibodies, with an overdose of ether. Tumors, liver, spleen, lungs, kidneys, and muscles (samples from four different locations in each rat) were then removed. In addition, ten separate lymph nodes were dissected (bilaterally the popliteal, inguinal and two axillary nodes, as well as one retroperitoneal and one node from the hilus of the liver). The bone marrow was aspirated

from the cut femoral bone with a sterile needle and syringe avoiding contamination. Samples of the marrow in the sternum was also taken. The rats were *not* bled and the different organs and tissues were *not* washed. Each tissue sample was weighed, m_j (g), and measured in an automatic NaI(Tl) gamma counter for radioactivity content, A_j (MBq).

The feasibility of tumor imaging with a scintillation camera with parallel holes or a pin hole collimator in different hosts was evaluated by inoculating 22 nude mice in parallel experiments with the same tumor suspension from the same passage as used in the nude rats. The mice were injected through the tail vein with the same labeled antibody 96.5, 4 μg (range 1.2-7.7 μg), and imaged and killed at intervals during 100 hr. Mice were dissected in the same way as the rats and radioactivity content measured in tissue.

Corrected Specific Tissue Uptake (STU_{corr})

The commonly calculated specific tissue uptake (STU), $A_{m,t}(^{125}I)$ for ^{125}I-96.5 MAb, is calculated by dividing A_j (^{125}I) with m_j, thus

$$A_{m,t}(125\ I) = A_j(125\ I)/m_j \qquad (MBq/g).$$

Knowing the ^{99m}Tc-RBC specific activity in the blood, A_m, blood (^{99m}Tc) and the total ^{99m}Tc-activity in the tissue $A_j(^{99m}Tc)$, then the mass of the blood m_{blood} is calculated by

$$^{m}blood = A_j\ (^{99m}Tc)/A_{m,blood}\ (^{99m}Tc)\ (g)$$

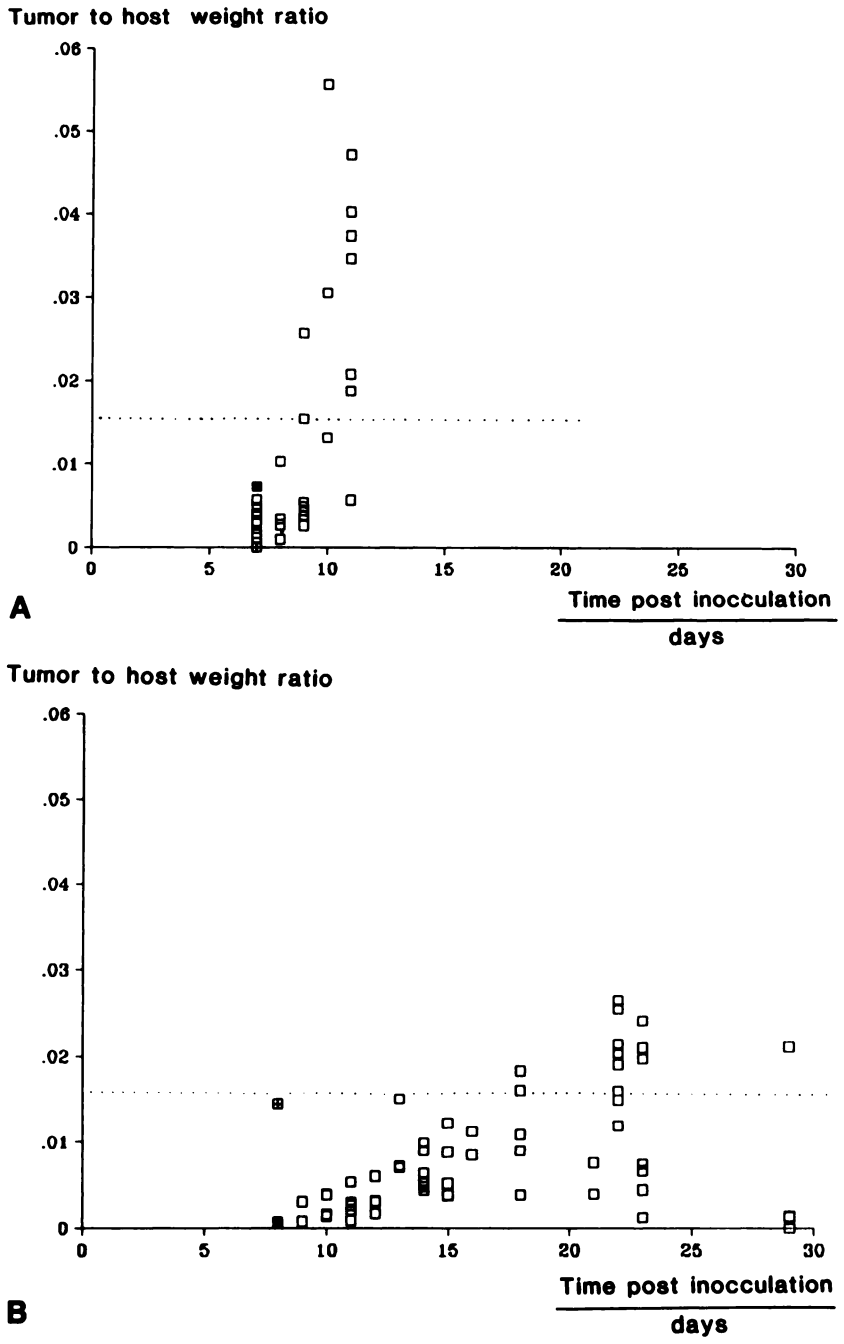

FIGURE 1
Tumor-to-host weight ratio after tumor inoculation for (A) nude mice and (B) nude rats. The dotted line represents the corresponding common final tumor burden of 1 kg in a patient of 70 kg body weight.

The blood activity in the tissue from ^{125}I-96.5 MAb, $A_{blood}(^{125}I)$, can then be evaluated when knowing the specific activity in the blood, Am,blood (^{125}I) as

$$A_{blood}\,(^{125}I) = A_{m,blood}\,(^{125}I) \times m_{blood}$$

The corrected specific tissue uptake (STU_{corr}) is then,

$$[A_{m,t}(^{125}I)]_{corr} = \frac{A_j(^{125}I) - A_{blood}(^{125}I)}{m_j - m_{blood}}.$$

This calculation takes two important factors into account, first the activity in the blood as a result of labeled antibodies, and second the mass of blood in each sample measured.

Blood Flow Measurements

Relative tumor and tissue blood flow in the nude rat was determined by injecting cerium-141- (^{141}Ce) labeled nonbiodegradable microspheres (16.5 μm, DuPont Company, No. Billerica, MA), through an intraarterial catheter through the carotid artery, with the tip of the catheter in the left ventricle of the heart. The spheres were injected during 20 sec. The animals were then killed and tumor and organs dissected and counted for activity uptake. Animals were excluded when a 20% difference in uptake between the kidneys was present. Blood flow values were calculated with reference to the renal values.

Scintillation camera measurements

The nude rat and the nude mouse models were compared with respect to in vivo detectability by imaging the animals using either a parallel hole (32,000 holes, low energy) or a pinhole collimator. A standard scintillation camera (General Electric Maxi Camera I, GE, Milwaukee, WI) was used connected to a computer for storage of images (Gamma 11, Digital Equipment Corp.). To compare the spatial resolution for the two collimators a line source phantom was imaged.

For ^{125}I- 96.5 MAb biokinetics, static images (sampling time 15 min) were taken at regulat intervals with the rat under ether anesthesia in supine position on the collimator face. A 25% energy window was centered over the 28-keV photo peak for ^{125}I. In the digital image, regions of interest (ROIs) were selected and the count rate subsequently estimated. The tumor uptake was calculated from the tumor ROI subtracted with background ROI normalized to the same area as the tumor, and divided by the total count rate (100%) in the rat. Background were selected over the muscles in the shoulder region with approximately the same muscle volume surrounding the tumor in the thigh.

Following labeling of the RBCs with ^{99m}Tc, an image of the blood pool was taken with the nude rat in the same position on the scintillation camera using a 25% energy window centered over the 140-keV photo peak.

The count rate in the 28-keV (^{125}I) window from ^{131}I was 6% of the count rate in the 365-keV (^{131}I) window for the parallel hole collimator.

RESULTS

Tumor

The mean life span of the nude rats is 4 mo. In our experiments, 2-mo-old rats were used. The mean survival time from inoculation of the tumor xenograft was 3 to 4 wk. The melanoma grafts used, retained their histology and antigenic activity through repeated passages (>10), and the tumor take was 100% without any pretreatment. The mean passage time was 2 wk.

All tumors in this experiment were from the same passage. The intramuscularly implanted tumors reached a median weight of 1.2 g (range 0.7-6.7; n = 17) and 1.8 g subcutaneously applied (range 0.6-4.4; n = 13) at the end of the experiments. In fast growing tumors necrosis was observed in their central parts. Some subcutaneously inoculated tumors grew invasively into the muscles. This explains the uneven numbers of s.c. and i.m. tumors.

Tumor to Host Weight Ratio

The final tumor burden in a patient seldom exceeds the ratio of 0.02. As shown in Fig. 1A and B, the tumor-to-host weight ratio in the nude rat resembles the human situation better than in the nude mouse, in which extreme ratios are reached rapidly. This enables more long lasting experiments in the nude rat, before the tumor has reached such a size the animal has to be killed.

Relative Tumor Blood Flow

A 20% difference was accepted between the two kidneys in the rat indicating an even distribution of the microspheres in blood from the heart. In Table 1 the blood flow measurements with ^{141}Ce microspheres (nine rats) relative to the kidneys are presented. The tumors had a higher blood flow than the resting muscle, but it was lower than other tissues measured.

In Vivo Imaging

In comparison between images of nude mice and nude rat inoculated with the same tumor suspension, injected with the same amount of labeled antibody (^{125}I-96.5) per gram animal, it was clearly seen that the larger nude rat was preferable to image, when the parallel hole collimator was used, and this enabled a quantification of the image.

TABLE 1
Relative Blood Flow Measured by Intracardial Injection of ^{141}Ce Microspheres in the Nude Rat Heterotransplanted with Malignant Melanoma (n = 9)

Organ	Mean ± s.d.	
Kidney*	1.00	
Lungs	0.42	0.30
Spleen	0.45	0.38
Liver	0.15	0.08
Tumor	0.11	0.07
Muscle	0.07	0.03

* Less than 20% difference was accepted between kidney values.

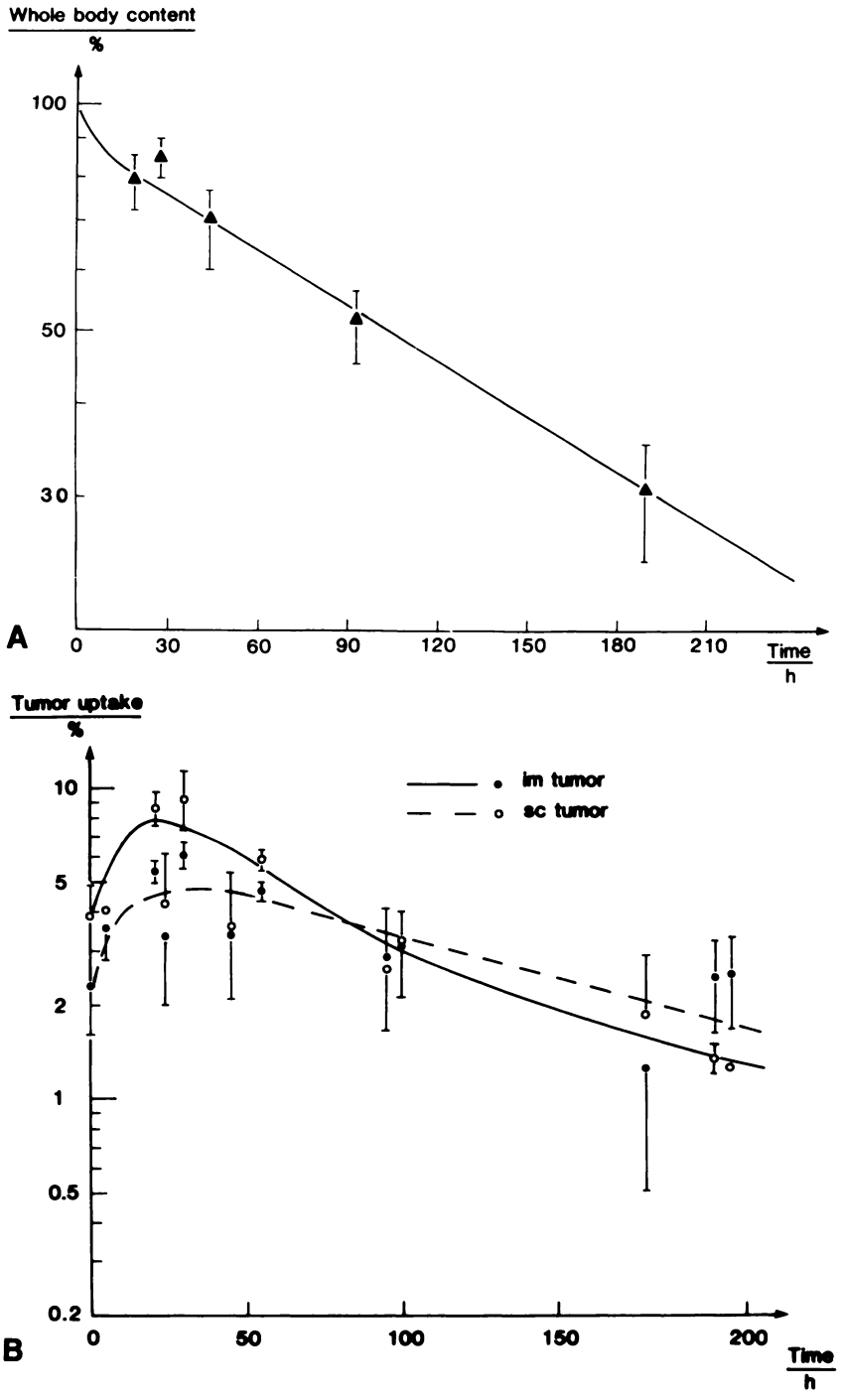

FIGURE 2
Biokinetics of ^{125}I-96.5 antibody measured in the scintillation camera images in the nude rat. (A) Whole body retention and (B) uptake in s.c. and i.m. tumors. Lines represents a fit, mean ± s.d. given in points with more than three observations.

In Vivo Biokinetics Measured by Scintillation Camera

The total-body retention of the ^{125}I-labeled whole antibody 96.5 is given in Figure 2A. The outflow can be described by a biexponential function. The uptake in the subcutaneous and intramuscular tumors as a function of time are given in Figure 2B.

Image Contrast

The contrast, calculated as T-B/B for the nude rats, is given in Figure 3A and B. During the first 50 hr an increase in the image contrast of a factor of approximately seven in magnitude was registered. The individual variations between different tumors were quite extensive as shown, by the s.d. values. No significant difference between the s.c. and i.m. tumor images could be recorded.

Specific Tissue Uptake of ^{125}I-96.5

The disappearance rates of ^{125}I-96.5 and ^{131}I-OKT3 from whole blood and plasma were identical as shown in Figure 4.

The specific tissue uptake for the different dissected

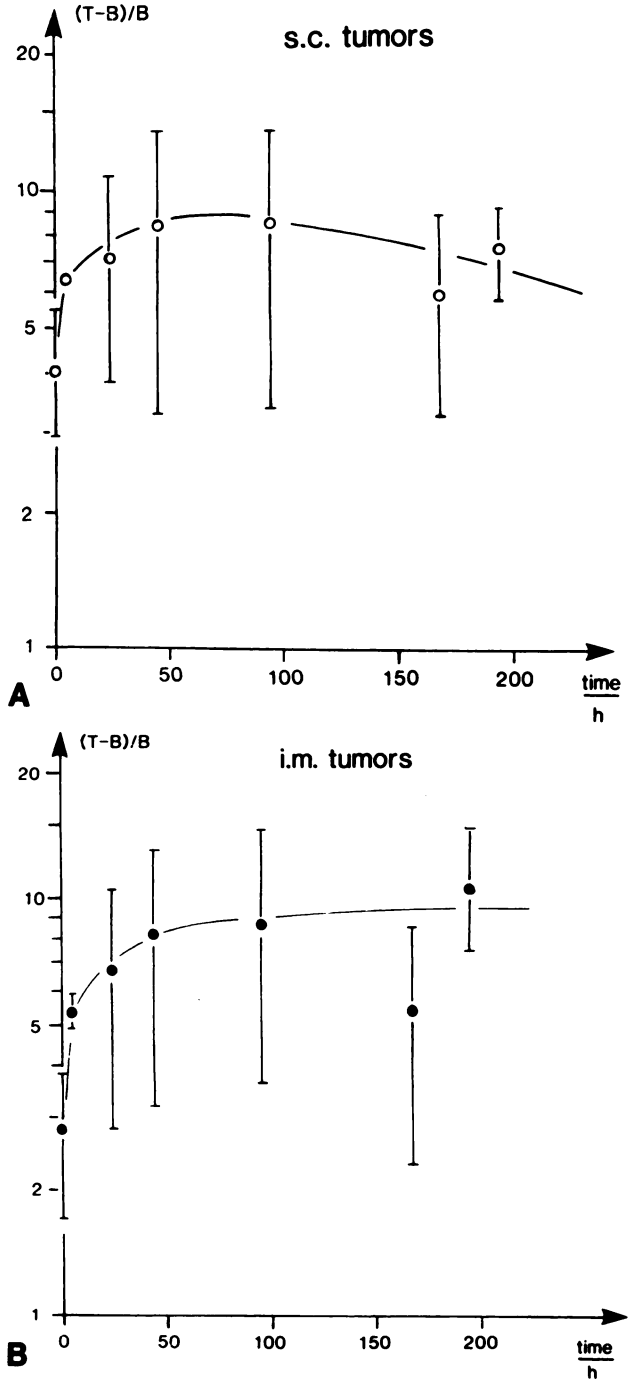

FIGURE 3
The time variation of contrast for the tumors evaluated in the scintillation camera images expressed as tumor to background count rate ratio for ^{125}I-96.5, in s.c. (A) and in i.m. (B) tumors after a period of 200 hr after antibody injection.

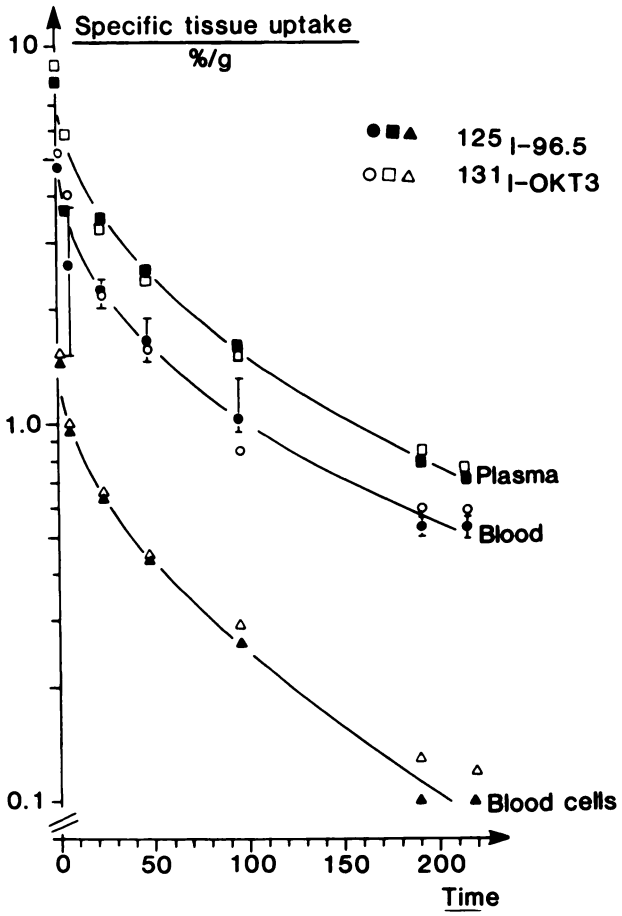

FIGURE 4
Specific activity of ^{125}I-96.5 (filled symbols) and ^{131}I-OKT3 (unfilled symbols) in plasma, whole blood and blood cells during 200 hr after i.v. injection in the nude rat.

tissues are given in Figure 5A and B. In the tumors, the uptake of antibody 96.5 reached a maximum after 30 hr, with peak values of 1.6%/g for i.m. tumors and 1.4%/g for s.c. tumors. Early high values were also recorded in the lungs, whereas the muscles showed the lowest activity (0.1% g).

Initially, the bone marrow specific tissue uptake (STU) was relatively high, higher than all other organs, but it then fell and after 30 hr it levelled out together with the other organs. The lymph glands, showed a slower initial increase than the other tissues and then remained relatively high. Liver, kidney, and spleen showed an intermediate accumulation. The muscle tissue, however, showed a constant STU of 0.1%/g of injected dose.

In the parallel experiments with the nude mouse model injected with the same ^{125}I-96.5 antibody the tissue/blood and tumor to tissue was in the same order as the rat. Table 2 shows the uptake ratio at 40 hr after i.v. injection.

Corresponding curves for the control monoclonal antibody OKT3 did not show any selectivity for the tumor and following the plasma clearance the uptake curves were parallel for all organs including the tumors (Fig. 5C and D). The disappearance rate in the bone marrow was equal for OKT3 and 96.5. The initial slow increase of specific tissue uptake in the lymph nodes were also similar for 96.5 and OKT3. The ratio over time between specific activity of MAb 96.5 and OKT3

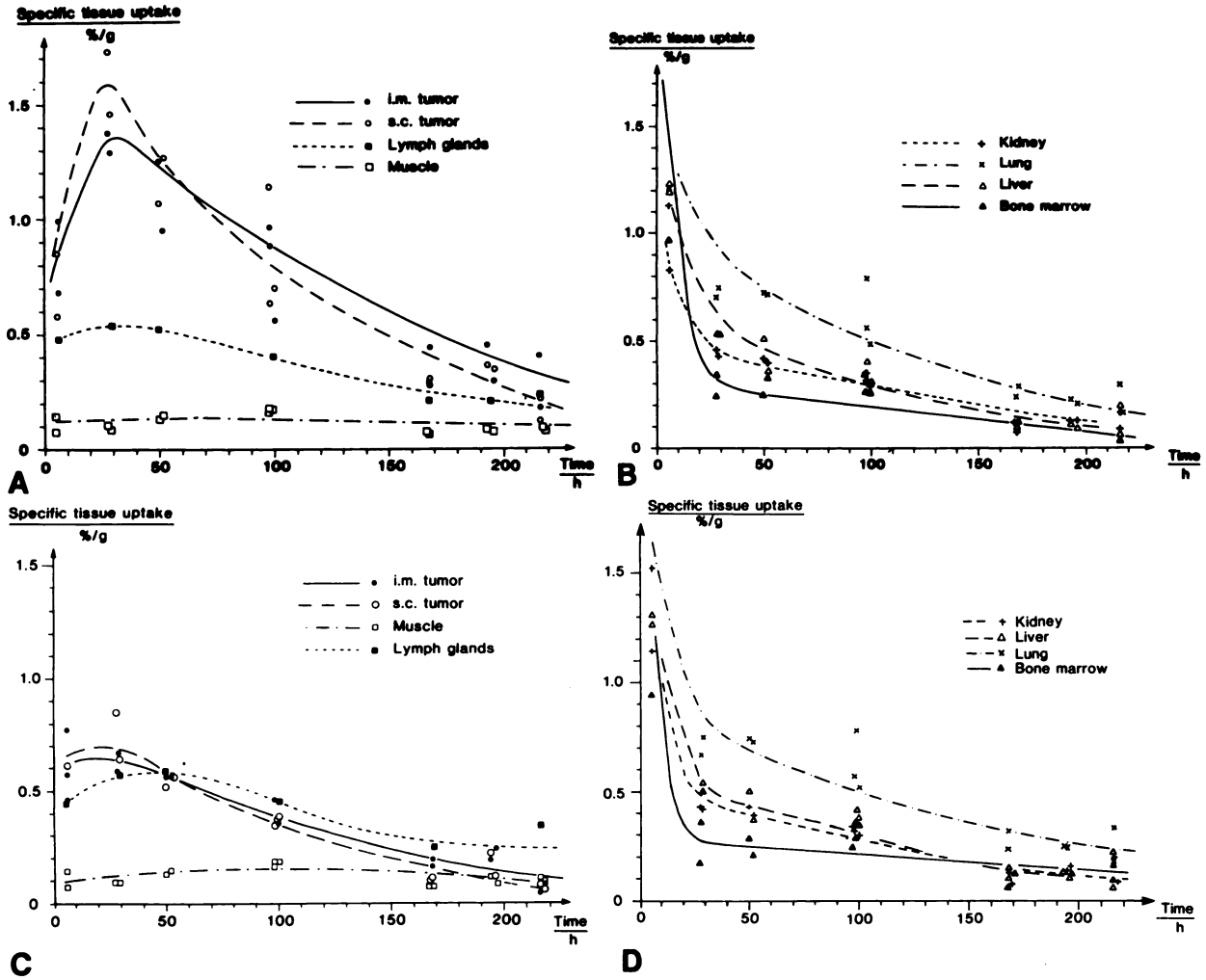

FIGURE 5
The time-activity curves (STU) for the specific tissue uptake of ^{125}I-96.5 (A, B) and ^{131}I-OKT3 (C, D) in the different dissected organs and tumors. For every ■ symbol average of ten lymph nodes, and for every □ symbol average of four muscle sample. Note the high initial uptake for the bone marrow and the different biokinetics for the lymph glands.

is shown in Figure 6. It clearly illustrates that for all other tissues than the tumor the ratio equals unity.

Corrected Specific Tissue Uptake (STU_{corr})

In Figure 7, the corrected specific tissue uptake (STU_{corr}) is shown. These tumor values compared to the STU-values, were only slightly influenced by this correction which implies that the main tumor activity (Fig. 5A and B) was truly bound and not emanating from the blood content of the tumor sample. In the liver and lungs, however, the STU_{corr}-values after 30 hr were reduced to ~20% of the uncorrected ones (Fig. 5 A and B). The correction did not seem to influence the initial high bone marrow values, but after 30 hr the STU_{corr} was very low. The uptake in the lymph glands was only reduced by 20% by the correction indicating that the main activity was bound to the tissue. The renal values have not been evaluated since the small amount of nonbound ^{99m}Tc is actively excreted in the urine making correction impossible.

In Figure 8 the corresponding corrected specificity of the labeled antibody uptake is shown as the ratio of corrected specific tissue uptake of specific and control antibody 96.5/OKT3. Here also the ratio equals unity for all organs except for the tumors in which a higher ratio was reached due to the specific binding of antibody 96.5.

DISCUSSION

As shown in Figure 1, even if the tumors in the rat and mouse grow at approximately the same rate, the tumor-to-host ratio is more favorable for the rat than for the mouse because of the larger size of the rat. High ratios (>0.02) are soon reached in the nude mouse and do not resemble the clinical situation.

TABLE 2
Specific Tissue Uptake of ^{125}I-Labeled Monoclonal Antibody 96.5 40 hr After i.v. Injection of the Nude Rat and in the Nude Mouse Heterotransplanted with Human Melanoma

	Nude mouse			Nude rat		
		Ratio			Ratio	
	%/g	Ti*/B‡	Tu†/Ti	%/g	Ti/B	Tu/Ti
Blood	9.00	—	0.70	1.90	—	0.74
Tumor	6.30	0.70	—	1.40	0.74	—
Lungs	4.30	0.48	1.47	0.82	0.43	1.71
Liver	3.75	0.42	1.68	0.51	0.27	2.75
Kidney	3.50	0.39	1.80	0.41	0.22	3.41
Muscle	1.70	0.19	3.70	0.12	0.06	11.7

* Tissue.
† Tumor.
‡ Blood.

The opportunity to use a parallel hole collimator for the larger nude rat facilitates the imaging procedure and gives a higher sensitivity and the images are more easily quantitated. Although the pinhole collimator showed the best spatial resolution—7 mm compared with 12 mm for the parallel hole collimator—the lower and nonhomogenous sensitivity of the pinhole collimator still makes it less favorable for in vivo imaging.

The retention of the whole antibody 96.5 and OKT3 in blood and plasma of the nude rat was identical as seen in Figure 4. There are no comparable OKT3-data for the nude mouse. However, it seems that the biologic half-life for whole antibodies was longer in the rat than the half-life reported in the nude mice even if the injected amount of antibody per gram animal was identical (*20*). As in the nude rat, the tumor-to-blood ratio of radiolabeled ^{125}I-96.5 in the mouse was never above unity (Table 2). This important factor limits the possibility for good imaging, but the size of the rat compensates for this, and good visibility of the tumors was obtained. In the parallel experiments where rats and mice were injected with the ^{125}I-96.5 antibodies, we found no difference between the tumor-to-organ ratios (Table 2). They were of the same order of magnitude as reported by other authors (*2,20*).

The relative uptake measured in the image for the different tumors showed a marked variation (Figs. 2B, 3A, and 3B). This fact appears to reflect the clinical situation in which the uptake in small tumors is often difficult to compare with the background activity. The variability does not seem to depend entirely upon the tumor size, but might also be a result of the presence of necrosis, heterogeneity, ischemia, and hypoxia. Hagan et al. found that the uptake per gram radiopharmaceutical in the tumor was inversely proportional to the tumor size in the nude mouse but local variations were found, probably because of necrosis in the tumor

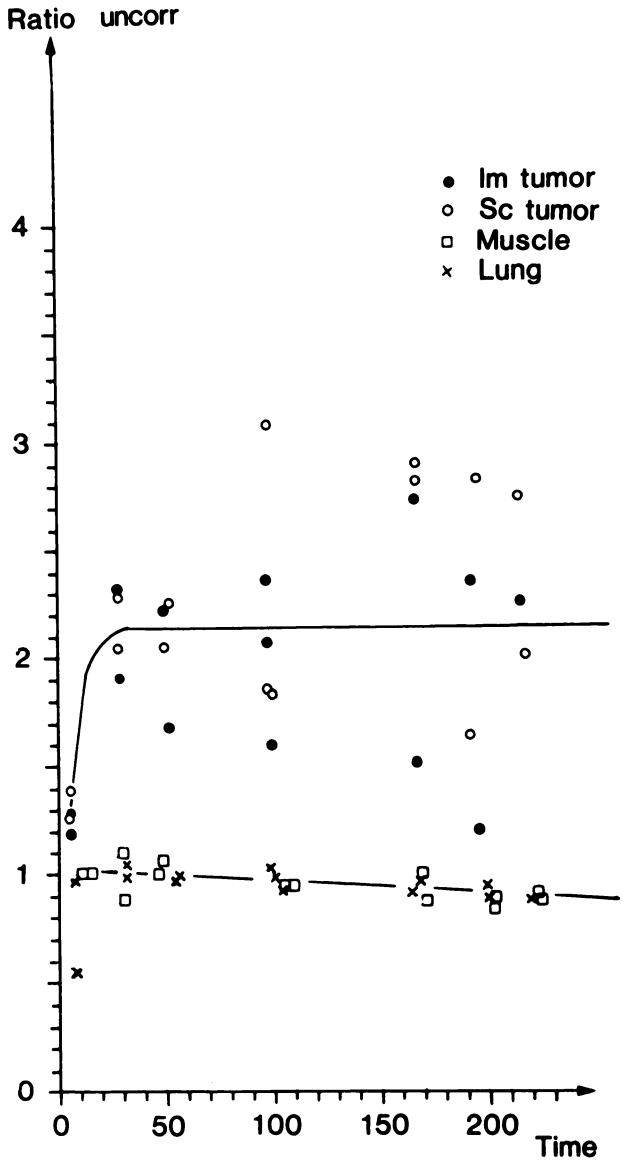

FIGURE 6
Ratio of specific tissue uptake of 96.5 and OKT3 in different organs and tumors in the nude rat. Note that all organs except the tumors have a ratio of one.

(*21*). In previous experiments, we have also noted this inverse relationship between tumor size and STU (Poster: Ydström, Strand, Ingvar. University of London, Hammersmith Hospital, June 1984). Other workers have not found any evidence that regional differences in blood flow and capillary permeability might influence the delivery of immunoglobulins to tumor tissue (*22*). However, Sands et al. found that the localization index was five times higher for subrenal than for subcutaneous tumors, and they explained this by differences in local blood flow (*23*). In our measurements with ^{141}Ce microspheres in rats of blood flow, there was a higher variation of blood flow in the intramuscular than in the subcutaneous tumors. The intra-

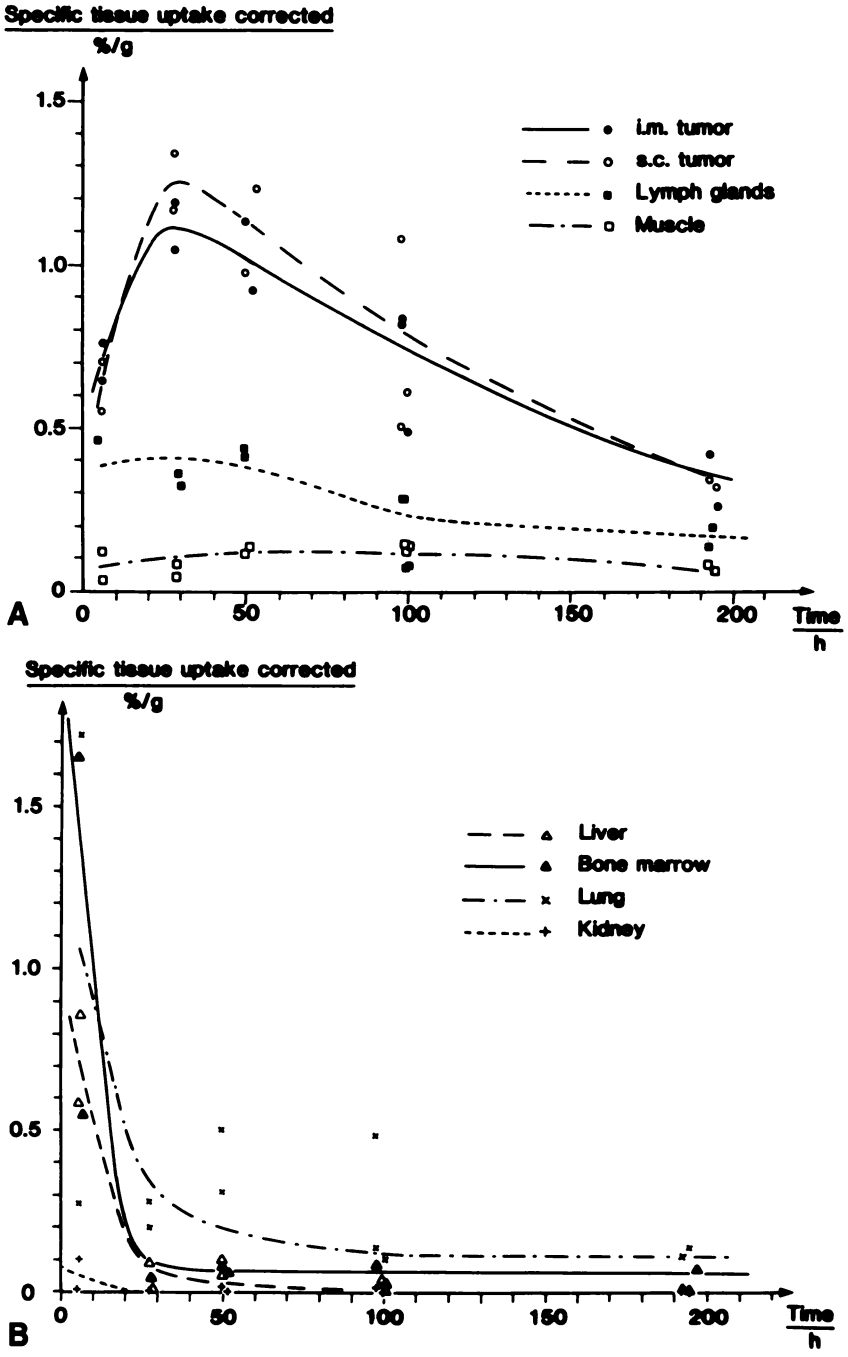

FIGURE 7
Corrected specific tissue uptake (STU_{corr}) of ^{125}I-96.5 in the different dissected organs and tumors in the nude rat, calculated from basic data in Figure 5 A, B and corrected for blood content of labeled antibody 96.5. Still there is a high uptake in the tumors compared to Figure 5 A, B but the STU_{corr} in other organs are low except for the lymph nodes that remains quite high.

muscular tumor varied more in size and showed a higher degree of necrosis in the larger tumors.

The ideal time for imaging depends on several factors including type of radioisotope, type and form of antibody molecules, and the characteristics of the target antigen. In the present study, the tumor contrast reached an optimum after ~40 hr, and it then tended to stay high during the whole observation time (200 hr). The specific tissue uptake in organs like liver, lung and spleen (Figs. 5 A and B) might indicate the presence of a low amount of tumor antigen or presence of Fc receptors in these tissues. The possibility of shed antigen p97, though not reported, causing the presence of labeled antibody in these organs may represent clearance by the reticuloendothelial system of antibody-antigen complexes (*24*).

When the corresponding in vivo and in vitro uptake values for the individual tumors were compared, it was found that there is a tendency to overestimate the uptake values in in vivo by the gamma camera. A linear regression for these values gives the relation, $y = 0.52x + 1.58$, where y is the percentage uptake in vivo and x the percentage uptake in vitro. This discrepancy was also found when in vivo images of rat thighs without

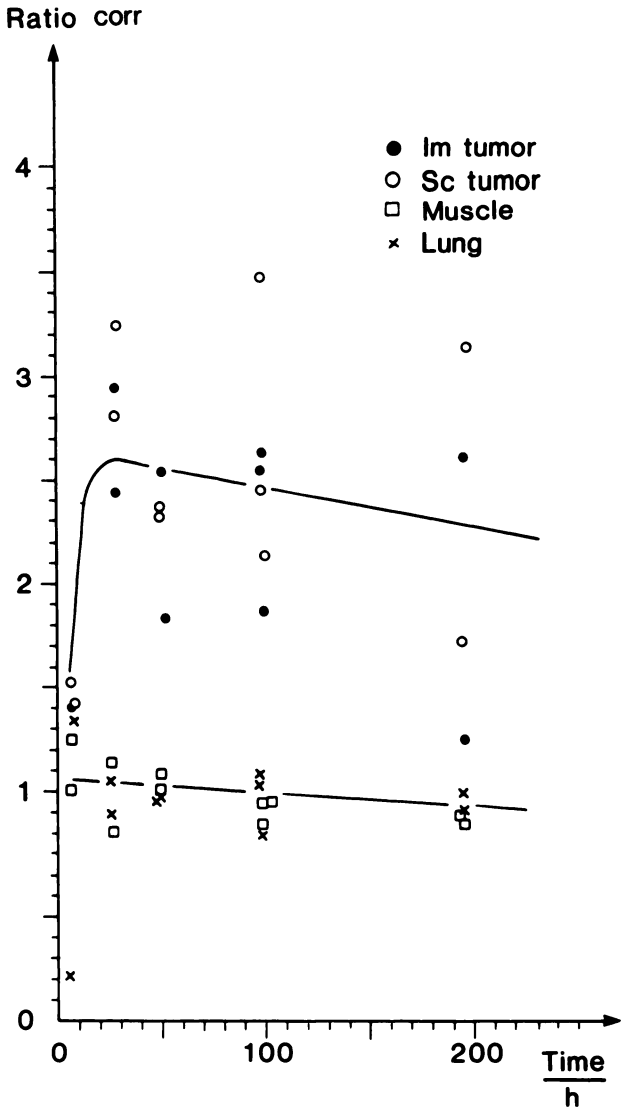

FIGURE 8
Ratio of corrected specific tissue uptake of 96.5 and OKT3 in different organs and tumors in the nude rat based on the data in Figure 7. Note that in comparison with Figure 6 the correction for blood content is only significant for the tumor values.

tumors were compared with thighs with tumors. During 0-48 hr, the used shoulder background values was underestimated by a factor of two, slightly more right after injection and somewhat less at 48 hr. This points out the necessity to select proper background areas. Still a degree of uncertainty exists and has to be regarded for every image study.

The lymph nodes showed a slower initial uptake relative to other organs and it did not parallel them or the blood until after 50 hr. This slower uptake might represent an alternative route of the antibodies to the nodes. Instead of mainly being taken up from the blood, the antibodies could penetrate the basal membrane and then be distributed via the interstitial fluid to the lymphatic ducts and the lymph nodes. The bone marrow showed a very high uptake immediately following the antibody injection. This finding, confirmed by others, is alarming from a clinical point of view. It has been hypothesized that the 100-nm openings characteristic of the sinusoidal blood vessels in the bone marrow, spleen and liver permit a very rapid access of antibodies to sites of binding and/or uptake (*25*).

The killing of the animals and the handling of the tissue samples for in vitro measurements of the relative activity is important. Few authors have reported their procedures in detail. Some workers bleed their animals to death and blot and rinse dissected tissues in saline (*2*). Such measures influence the measurements. We propose instead the described correction method where the specific activity of the remaining blood could be calculated for every tissue sample and subtracted.

The corrected specific tissue uptake appears to yield a more accurate evaluation of the biodistribution for the radiolabeled antibody in the different tissues (Fig. 7). This is most evident when looking at the blood rich liver, where the activity was reduced to 20% at 30 hr and to ~0 after 90 hr. This implies that the activity found in the liver represented mainly that of the circulating blood. The initial high uptake in the liver, however, could be the result of an accumulation in the reticuloendothelial system by a relative initial overload of antibodies and the clearance of damaged labeled protein and immune complexes. The lungs, however, still showed a high uptake after correction (tumors excluded), which indicates some binding of antibodies to lung tissue or trapping of immune complexes there. These two speculations have to be further investigated. There was no significant difference in the STU and STU_{corr} in the tumors implanted subcutaneously or intramuscularly, showing that the main part of the activity registered was bound.

As far as we now know, there are several factors in addition to immunologic ones that account for the antibody localization to the tumor. These additional factors include, e.g., the dehalogenation of iodinated antibodies, tumor vascular permeability, and blood flow. They must be identified both in animal models and in humans before any animal model should be considered reliable and used for predicting the efficacy of radiolabeled antibodies for diagnosis and therapy.

In conclusion, we fund the nude rat model superior to the nude mouse model for investigating all these important factors which have been intensely discussed in recent years. We should especially like to emphasize the advantages of calculating the corrected specific tissue uptake in vitro in order to achieve a quantitative estimate of tissue antibody uptake. Also the antibody biokinetics for the bone marrow and lymph glands has shown that these organs should be carefully considered when monoclonal antibodies are evaluated for clinical

use. Further studies in our model are under way concerning subcutaneous and regional injection of MAbs, compartment analysis, and dosimetry studies for therapeutic applications (*26*).

ACKNOWLEDGMENTS

This work was supported by the Swedish Medical Research Council (Project B86-16X-06573-04B), Swedish Cancer Society (Project 1625-B83-01X), the Åke Wiberg Foundation, Stockholm, the Medical Faculty, Lund, the John and Augusta Perssons Foundation for Medical Research, Lund, and the Royal Physiographic Society, Lund. The authors thank Karin Wingårdh and Eva-Cecilia Persson for technical assistance.

REFERENCES

1. Korsgaard R, Lindén C-L, Willén R, Willén H, Svensson G, Simonsson BG. Propagation of poorly differentiated human pulmonary adenocarcinoma in the nude athymic rats. *Int J Cancer* 1983; 32:793–799.
2. Beaumier PL, Krohn KA, Carrasquillo JA, et al. Melanoma localization in the nude mice with monoclonal Fab against p97. *J Nucl Med* 1985; 26:1172–1179.
3. Buchsbaum O, Randall B, Hanna D, Chandler R, Loken M, Johnson E. Comparison of the distribution of binding of monoclonal antibodies labelled with ^{131}iodine or ^{111}indium. *Eur J Nucl Med* 1985; 10:398–402.
4. Colcher D, Zalutsky M, Kaplan W, Kufe D, Austin F, Schlom J. Radiolocalization of human mammary tumours in athymic mice by a monoclonal antibody. *Cancer Res* 1983; 43:736–742.
5. Ghose T, Kulkaemi N, Ferrar S, Norvell BT, Kulkarmi P, Blair AH. Imaging human tumours in nude mice. In: Rhodes B, Burchiel S, eds. *Radioimmunoimaging and radioimmunotherapy.* Elsevier, Amsterdam, 1983, pp 255–263.
6. Hwang KM, Fodstad Ö, Oldham RK, Morgan AC. Radiolocalization of xenografted human malignant melanoma by monoclonal antibody (9.2.27) to melanoma-associated antigen in the nude mice. *Cancer Res* 1985; 45:4150–4155.
7. Mach JP, Buchegger F, Forni M, et al. Use of radiolabelled monoclonal anti-CEA antibodies for the detection of human carcinoma by external photoscanning and tomoscintigraphy. *Immunol Today* 1981; 239–249.
8. Lotze MT, Carrasquillio JA, Weinstein JN, et al. Monoclonal antibody imaging of human melanoma. *Ann Surg* 1986; 223–235.
9. Moldofsky PJ, Powe J, Mulhern CB, et al. Metastatic colon carcinoma detected with radiolabelled F(ab')$_2$ monoclonal antibody fragments. *Radiology* 1983; 149:549–555.
10. Murray JL, Rosenblum MG, Sobol RE, et al. Radioimmunoimaging in malignant melanoma with ^{111}In-labelled monoclonalantibody 96.5. *Cancer Res* 1985; 45:2376–2381.
11. Pateisky N, Phillip K, Skodler WD, Czerwenka K, Hamilton G, Burchell J. Radioimmunodetection in patients with suspected ovarian cancer. *J Nucl Med* 1985; 26:1369–1376.
12. Giovanella BC, Stehlin JS, Coil D. Human tumours heterotransplanted in nude mice and rats. *Expl Cell Biol* 1984; 52:76–79.
13. Brown JP, Woodbury RG, Hart CE, Hellström I, Hellström K-E. Quantitative analysis of melanoma associated antigen p97 in normal and neoplastic tissues. *Proc Nat Acad Sci USA* 1981; 78:539–543.
14. Ey PL, Prawse SJ, Jenkins CR. Isolation of pure IgG, IgG2b immunoglobulins from mouse serum using protein A Sepharose. *Immunohistochemistry* 1978; 15:429–436.
15. Reinherz EL, Schlossman SF. The differentiation and function of human T-lymfocytes. *Cell* 1980; 19: 821–827.
16. Brodin T, Jansson B, Hedlund G, Sjögren H-O. Use of a monoclonal rat anti-mouse IgG light chains (RAMOL-1) antibody reduces background binding in immunohistochemical and fluorescent antibody analysis. *J Histochem Cytochem* 1988: in press.
17. Brown JP, Nishiyama K, Hellström I, Hellström K-E. Structural characterization of human melanoma associated antigen p97 using monoclonal antibodies. *J Immunol* 1981; 127:539–546.
18. Ferens JM, Krohn KA, Beaumier PL, et al. Highlevel iodination of monoclonal antibody fragments for radiotherapy. *J Nucl Med* 1984; 25:367–370.
19. Pavel DG, Zimmer AM, Patterson VN. In vivo labelling of red blood cells with ^{99}Tc^{m}. A new approach to blood pool visualization. *J Nucl Med* 1977; 18:305–308.
20. Larson SM, Brown JP, Wright PW, Carrasquillo JA, Hellström I, Hellström K-E. Imaging of melanoma with ^{131}I-labelled monoclonal antibodies. *J Nucl Med* 1983; 24:123–129.
21. Hagan PL, Halperin SE, Dillman RO, et al. Tumour size; effect on monoclonal antibody uptake in tumour models. *J Nucl Med* 1986; 27:422–427.
22. Blasberg RG, Nakagawa H, Bourdon MA, Groothvis DR, Patlak CS, Bigner DD. Regional localization of a glioma-associated antigen defined by monoclonal antibody 81C6 in vivo: kinetics and implications for diagnosis and therapy. *Cancer Res* 1987; 47:4432–4443.
23. Sands H, Jones PL, Neacy WP, Shah SA, Gallagher BM. Siterelated differences in the localization of the monoclonal antibody OX7 in SL2 and SL1 lymphomas. *Cancer Immunol Immunotherapy* 1986; 22:169–175.
24. Rosenblum MG, Murray JL, Haynie TP, et al. Pharmacokinetics of ^{111}In-labelled anti-p97 monoclonal antibody in patients with metastatic malignant melanoma. *Cancer Res* 1985; 45:2382–2386.
25. Weinstein JN, Eger RR, Covell DG, et al. The pharmacology of monoclonal antibodies. *Ann New York Acad Sci* 1978; 507:199–210.
26. Strand S-E, Norrgren K, Ingvar C, Brodin T, Hallstadius L, Ljungberg M. Parameters required in a dose planning model for radioimmunotherapy. In: *Radionuclides for therapy.* Böttsteiner Colliquium IV, June 13-14, 1986.